A Posttranslational Modification of β-Actin Contributes to the Slow Dissociation of the Spectrin-Protein 4.1–Actin Complex of Irreversibly Sickled Cells

Archil Shartava,* Carlos A. Monteiro,* F. Aladar Bencsath,‡ Klaus Schneider,¶ Brian T. Chait,¶ Rick Gussio,* Linda A. Casoria-Scott,* Arvind K. Shah,§ Christine A. Heuerman,* and Steven R. Goodman*‖

Departments of *Structural and Cellular Biology, ‡Biochemistry, §Mathematics and Statistics, and ‖USA Comprehensive Sickle Cell Center, University of South Alabama College of Medicine, Mobile, Alabama 36688; ¶Mass Spectrometry Laboratory, The Rockefeller University, New York 10021; and **Frederick Biomedical Supercomputer Center, National Cancer Institute-Frederick Cancer Research and Development Center, PRI/Dyn Corp., Frederick, Maryland 21702

Abstract. Irreversibly sickled cells (ISCs) remain sickled even under conditions where they are well oxygenated and hemoglobin is depolymerized. In our studies we demonstrate that triton extracted ISC core skeletons containing only spectrin, protein 4.1, and actin also retain their sickled shape; while reversibly sickled cell (RSC) skeletons remodel to a round or biconcave shape. We also demonstrate that these triton extracted ISC core skeletons dissociate more slowly upon incubation at 37°C than do RSC or control (AA) core skeletons. This observation may supply the basis for the inability of the ISC core skeleton to remodel its shape. Using an in vitro ternary complex dissocia-tion assay, we demonstrate that a modification in β-actin is the major determinant of the slow dissociation of the spectrin-protein 4.1–actin complex isolated from the ISC core skeleton. We demonstrate that the difference between ISC and control β-actin is the inaccessibility of two cysteine residues in ISC β-actin to labeling by thiol reactive reagents; due to the formation of a disulfide bridge between cysteine^{284} and cysteine^{373} in ISC β-actin, or alternatively another modification of cysteine^{284} and cysteine^{373} which is reversible with DTT and adds less than 100 D to the molecular weight of β-actin.

THE molecular events which occur within red blood cells (RBCs)[1] from homozygous sickle cell (SS) patients, and to their extracellular environment, leading to the painful sickle cell crisis, organ damage, and mortality have been of great interest to the clinical and scientific community (reviews Hebbel, 1990, 1991; Powers, 1990; Francis and Johnson, 1991; Joiner, 1993). Blood from SS patients can be separated on density gradients into morphologically and physiologically distinct RBC classes (Fabry et al., 1984). During the course of vasoocclusion the highest density class of RBCs are selectively trapped in the microvasculature (Kaul et al., 1986, 1989). This high-density class

1. *Abbreviations used in this paper*: CFF, class II force field; CF-FAB, continuous flow fast atom bombardment; DTNB, 5,5'-dithiobis-(2-nitrobenzoate); FAB-MS, FAB mass spectrometry; HDSS, high density SS; IOV, inside-out vesicles; ISC, irreversibly sickled cell; LDSS, low density SS; MALDI, matrix-assisted laser desorption ionization; MD, molecular dynamics; RBC, red blood cell; RSC, reversibly sickled cell; TOF, time of flight; USD, unsickleable SS dense discocytes.

of RBCs includes irreversibly sickled cells (ISCs) (60–85%) that retain a sickled shape in well oxygenated blood, and unsickleable SS dense discocytes (USDs) (Kaul et al., 1983). These observations explain why ISCs and USDs are reduced in the peripheral blood during a sickle cell crisis (Fabry et al., 1984; Ballas et al., 1988; Lande et al., 1988; Ballas and Smith, 1992). The ISCs appear to block the narrowed lumen of vessels lined primarily with the more adherent lower density reversibly sickled cells (RSCs), and sometimes by direct capillary occlusion (Kaul et al., 1989; Fabry et al., 1992).

Eighteen years ago, Lux and co-workers made the important observation that most rbc membranes (ghosts) isolated from ISCs remain sickled, and triton skeletons prepared from ISC ghosts all remain sickled (Lux et al., 1976). These observations demonstrated that after removal of all of the hemoglobin (HbS) from the ISC RBC, and most of the membrane phospholipids and integral membrane proteins, the remaining skeleton retained the sickled shape. When sickled RSC's were triton extracted the resulting skeletons did not retain their sickled shape. For the released skeletons to remodel their shape, protein associations between spectrin, protein 4.1, and actin protofilaments (and other accessory

proteins) must be dissociated, and then new interactions formed. The experiments described in this article demonstrated that ISC core membrane skeletons (containing only spectrin, protein 4.1, and actin) dissociate slowly, and this slow dissociation is due, in part, to a posttranslational modification in ISC β-actin.

The RBC contains a two-dimensional latticework of fibrous proteins which covers the cytoplasmic surface of its plasma membrane. This supramolecular structure, termed the membrane skeleton, maintains the biconcave shape of the erythrocyte, gives it essential properties of elasticity and flexibility for its circulatory travels, controls the lateral mobility of integral membrane proteins, and serves as a structural support for the bilayer (for review see Goodman et al., 1988). The essential core components of this two dimensional meshwork are spectrin, f-actin, and protein 4.1 (Yu et al., 1973; Sheetz, 1979), although triton membrane skeletons isolated at moderate ionic strength conditions (such as those used by Lux et al., 1976) contain other more minor components which will be described below.

Erythrocyte spectrin is primarily an $(\alpha\beta)_2$ tetrameric flexible rod of 200 nm extended contour length, formed by head-to-head linkage of two $\alpha\beta$ heterodimers (Shotton et al., 1979). Cloning and cDNA sequencing of both the α subunit (Sahr et al., 1990) and β subunit (Winkelman et al., 1990) have indicated molecular weights of 280 kD (α) and 246 kD (β) for the spectrin subunits. Essential to the formation of the two-dimensional membrane skeleton is the ability of spectrin tetramers to bind actin filaments at both ends, thereby cross-linking f-actin (Brenner and Korn, 1979; Cohen et al., 1980; Shen et al., 1986). The actin binding domain of human RBC spectrin has been localized to a stretch of 140 amino acids at the NH_2 terminus of β spectrin from alanine[47] through lysine[186] (Karinch et al., 1990). Erythrocyte actin protofilaments observed on electron microscopy of negatively stained intact membrane skeletons fall within a narrow range of lengths, with a mean length of 33 to 37 nm in control (AA)RBCs, equivalent to a double-stranded helix with ~14 actin monomers (Shen et al., 1986; Byers and Branton, 1985). The extended skeleton appears to be primarily a hexagonal lattice (Liu et al., 1987) with actin protofilaments (and associated proteins) at the center and six corners of the hexagons, interconnected by spectrin tetramers (~85%) and three armed hexamers (~10%). The spectrin–actin interaction is strengthened by a peripheral membrane protein, protein 4.1, which also binds to the ends of the spectrin tetramers (Tyler et al., 1979; Ungewickell et al., 1979; Fowler and Taylor, 1980). Therefore spectrin, actin protofilaments, and protein 4.1 constitute the core RBC skeleton.

Other accessory proteins to the skeleton include protein 4.9 which bundles f-actin in vitro (Siegel and Branton, 1985), tropomyosin which lines the grooves of actin protofilaments (Fowler and Bennett, 1984), and adducin a Ca^{2+}-calmodulin binding protein which stimulates the addition of spectrin to f-actin in a protein 4.1–independent manner (Gardner and Bennett, 1987; Mische et al., 1987). The spectrin membrane skeleton is attached to the membrane by at least two types of interactions. Ankyrin binds to β spectrin ~20 nm from the junction of the heterodimers and also binds to the integral membrane protein band 3 (Bennett and Sten-

buck, 1979, 1980; Yu and Goodman, 1979; Hargreaves et al., 1980; Wallin et al., 1984). The second membrane linkage is based on the ability of protein 4.1 to bind to an integral membrane protein (Shiffer and Goodman, 1984) which appears to be glycophorin C (Mueller and Morrison, 1981).

Previous attempts to look at membrane skeletal defects within the sickle cell have focussed on the membrane linkage proteins. Platt et al. (1985) demonstrated that SS spectrin depleted inside-out vesicles (IOVs) bound ~50% less spectrin in vitro than did control AA IOV. While this suggested a potential ankyrin defect, purified ISC ankyrin bound spectrin normally in vitro. Schwartz et al. (1987) demonstrated that SS protein 4.1 was more aggregated upon isolation than AA protein 4.1, and bound protein 4.1-depleted IOVs less effectively than AA IOV's. While both of these studies point to potentially important alterations in the linkage between the core skeleton and the SS bilayer, neither could explain the persistently sickled membrane skeleton observed on Triton X-100 extraction of ISC ghosts (Lux et al., 1976). In the triton-extracted skeletons the bilayer has been removed, yet the ISC skeleton remained sickled.

Hebbel et al. (1982) have demonstrated that sickle cells generate about twice the amount of activated oxygen species found in normal RBCs. The basis for this increase in oxygen radicals is the combined result of accelerated autoxidation of HbS to methemoglobin, a conversion which causes a release of heme (Hebbel et al., 1988). Heme is increased in content on the cytoplasmic surface of sickle cell membranes, and this increase correlates with the amount of membrane protein thiol modification (Kuross et al., 1988). It is therefore not surprising that spectrin, band 3, ankyrin, and protein 4.1 all have some degree of thiol modification (Rank et al., 1985; Schwartz et al., 1987). While the thiol modifications of spectrin and ankyrin are reversible with DTT (Rank et al., 1985), the oxidation of thiols in protein 4.1 is not reversible (Schwartz et al., 1987). Schwartz et al. (1987) have reported that SS protein 4.1 contains 1–2 mole % fewer cysteine than control protein 4.1, and 1 mole % cysteic acid not found in control protein 4.1. These studies raise the question of whether thiol oxidation of skeletal proteins may be involved in the persistently sickled shape of the ISC membrane skeleton.

In the current study we utilize an in vitro spectrin-4.1-f-actin ternary complex dissociation assay to demonstrate that ISC β-actin in the major cause of the slow dissociation of the persistently sickled ISC core skeleton. Using a combined protein chemistry, thiol labeling, and sophisticated mass spectrometry approach we demonstrate that ISC β-actin has a unique modification when compared to RSC or AA β-actin. This posttranslational modification in ISC β-actin appears to be the formation of a disulfide bridge between cysteine[284] and cysteine[373], or alternatively another modification of these cysteines which is reversible with DTT and adds less than 100 D to the molecular weight of β-actin. Therefore reversible thiol modification of β-actin leads to slow dissociation of the ISC membrane skeleton, which offers a reasonable explanation for the inability of the ISC skeleton to rapidly remodel when it is released from the bilayer. Additional protein components not present in the core skeletons, may participate in the slow remodelling of the ISC membrane skeleton in vivo.

Materials and Methods

Preparation of Density Separated RBCs, Ghosts, and Core Skeletons

Blood (20–30 ml) was obtained by venipuncture from homozygous SS subjects, sickle cell trait subjects, and AA control subjects in vacutainer tubes containing 143 USP units of lithium heparin. Fresh blood (5 ml/gradient tube) was placed over a six layer step gradient (5 ml/layer) composed of 45, 50, 55, 60, 65, and 70% Percoll in 18% Renografin M-60, 20 mM Hepes, 1 mM $MgCl_2$, 1 mM glucose (pH 7.4). Sedimentation was performed by centrifugation at 1,500 g for 45 min. Each cell fraction within the Percoll layers was removed without cross-contamination and then washed two times in 10 mM $NaPO_4$, 150 mM NaCl, pH 7.6.

Packed RBCs were lysed in 30 ml of ice cold lysis buffer (5 mM $NaPO_4$, 1 mM EDTA, pH 7.6) and ghosts sedimented at 31,000 g for 15 min at 4°C. This procedure was repeated until the pellet became white or light pink.

Freshly prepared ghosts (1 vol) were incubated on ice for 15–30 min in 9 vol of 10 mM $NaPO_4$, 0.6 M KCl, 1 mM ATP, 1 mM DFP, 1% Triton X-100, pH 7.6. In some cases skeletons were sedimented at 35,000 g for 45 min at 4°C, but not for immunofluorescence.

Immunofluorescent Images of Core Skeletons

Poly-L-lysine (0.1% in dH_2O) was applied to precleaned glass slides which were left to dry at room temperature. To 1 vol of RBC core skeletons was added one volume of 4% formaldehyde, 1.25% glutaraldehyde in PBS (150 mM NaCl, 10 mM $NaPO_4$, pH 7.6), and the mixture was incubated for 5 min at 22°C. Fixed skeletons were allowed to settle on poly-L-lysine glass slides for 5 min, and nonadherent skeletons were removed by three washes with PBS + 1% BSA. Primary antibodies prepared in rabbits against chicken muscle actin (Sigma Immunochemical, St. Louis, MO) and human rbc spectrin (characterized in Goodman et al., 1981) were diluted 1:100 in PBS + 1% BSA and applied to skeletons for 15 min at 22°C. After three washes for 5 min each in PBS + 1% BSA, FITC-conjugated goat anti–rabbit IgG (1:100 in PBS + 1% BSA) was applied to the skeletons for 15 min. Nonbound secondary antibody was removed by three washes in PBS + 1% BSA. The fluorescent skeletons were mounted and observed with a Leitz Dialux Fluorescent Microscope.

Isolation of Spectrin, Actin, and Protein 4.1

RBC core skeleton pellets were dissociated by incubation in 5 vol of 2 M Tris, pH 7.2, at 37°C for 30 min followed by sedimentation of undissociated material at 32,000 g for 30 min (4°C). The supernatant was layered onto a Sepharose 4B gel filtration column (1.5 × 170 cm) which had been equilibrated with 2 M Tris, 0.2 mM ATP, pH 7.2. The spectrin, protein 4.1, and actin were eluted with this same buffer and collected in 2 ml fractions. Every fraction following the void volume (∼50 ml) was analyzed by SDS-PAGE. Spectrin and protein 4.1 were dialyzed against 5 mM Tris, 0.5 mM NaN_3, pH 7.8. Actin was dialyzed against 2 mM Tris, 0.4 mM ATP, 0.5 mM NaN_3 ± 0.2 mM DTT (pH 7.8). All proteins were dialyzed with three changes every 12 h of 2 liters dialysis buffer and then concentrated to 1 mg/ml spectrin, 400 µg/ml actin, 500 µg/ml protein 4.1. Skeletal proteins were stored at 4°C and used within 48 h of isolation.

SDS-PAGE

SDS-PAGE was performed using the discontinuous buffer system of Laemmli (1970) and a 9% polyacrylamide separating gel. Protein was detected with Coomassie brilliant blue and densitometry performed with a Zeineth laser densitometer (Biomed Instruments, Inc., Fullerton, CA).

In Vitro Ternary Complex Dissociation Assay

Our procedure is a modification of published ternary complex assays (Ungewickell et al., 1979; Cohen et al., 1980). Purified spectrin (400 µg/ml), protein 4.1 (80 µg/ml), and g-actin (160 µg/ml) were incubated in 190 µl of polymerization buffer (4 mM Tris, 0.2 mM ATP, 0.5 mM NaN_3, 2 mM $MgCl_2$, pH 7.4) for 1 h at 22°C. The resulting ternary complexes were sedimented at 100,000 g for 30 min (4°C) and resuspended in 190 µl of high ionic strength triton buffer (10 mM $NaPO_4$, 0.6 M KCl, 1 mM ATP, 0.1 mM DFP, 1% Triton X-100, pH 7.6). The ternary complexes were allowed

to dissociate in this buffer at 37°C for 30 min followed by centrifugation at 100,000 g for 30 min. The resulting pellets were analyzed by SDS-PAGE and laser densitometry. Purified spectrin, protein 4.1, and nonpolymerized g-actin (not complexed) demonstrate minimal (<10%) sedimentation at 100,000 g (30 min) with no difference between control and sickle cell proteins.

The statistical analysis was done using a commercially available statistical software package, SAS (Statistical Analysis System). The descriptive statistics like mean, range, and standard errors were compiled for each of the eight combinations of actin, spectrin, and 4.1. The one-way analysis of variance was performed to compare the means of these combinations. Once the difference among means was established, the Duncan's multiple range test was performed to test for pairwise differences. The statistical discussion on these techniques can be found in Montgomery (1991).

Determination of Exposed Thiols with DTNB

The number of exposed thiol groups were measured with DTNB (Ellman, 1958). The reaction was monitored by spectrometry at 412 nm using the extinction coefficient of the thiobenzoate ion (13,600 M^{-1} cm^{-1}). The reaction was started by adding a 10-fold excess of DTNB to actin (1.5 × 10^{-5} M) and a reference cuvette in 2 mM Tris, 0.2 mM ATP, 0.5 mM NaN_3, pH 7.8. The reaction at 22°C was recorded over time on an LKB spectrophotometer. In some experiments the actin was reduced by dialyzing against 2 mM Tris, 0.2 mM ATP, 0.2 mM DTT, 0.5 mM NaN_3, pH 7.8, for 12 h, and then twice for 12 h against the same buffer without DTT.

Reverse Phase HPLC of Actin Digests

AA, HDSS, and LDSS β-actin was dialyzed against 75 mM NH_4HCO_3, 0.1 mM $CaCl_2$, pH 7.8. β-Actins (400 µg/ml) were incubated with trypsin at 50/1 (mol/mol) for 20 h at 37°C. Digested actin was dried to a powder in a Speed-Vac (Savant Instruments, Inc., Farmingdale, NY), and then resuspended in half the original volume with buffer A (0.1% trifluoroacetic acid [TFA] in HPLC quality H_2O). The actin digest (200 µg) was loaded onto a ODS 5 µ C_{18} reverse phase column (4.6 mm × 15 cm) with precolumn and eluted using a Beckman System Gold HPLC. The column was washed 5 min with buffer A, followed by a gradient of 0–100% buffer B (0.1% TFA, 80% acetonitrile) over 90 min. The flow rate was 1 ml/min and OD_{215} was monitored. Fractions (1 ml) were collected and dried in a Speed-Vac (Savant Instruments, Inc.) prior to mass spectrometry.

Each of the dried HPLC fractions were dissolved in 15 µl supporting fluid (methanol/glycerol/water 1:1:8) that contained 0.1% TFA. The injector for FAB-MS was loaded using 2.5 µl sample volumes, and injections were made in 10 scan intervals. The injector was carefully flushed with supporting fluid between samples (2 × 4 µl before loading, 2 × 4 µl after injection).

Mass Spectrometry

FAB-MS. A VG 70-250 SEQ hybrid tandem instrument equipped with a saddle-field FAB gun and a continuous flow-fast atom bombardment (CF-FAB) probe was used for the MS analyses. The probe was modified by attaching a micro-sampler injector (Rheodyne model 7520; Alltech Assoc., Inc., Houston, TX) to it on a mounting plate fastened to the handle. The original 0.5 µl sample volume of the injector was increased to about 1.8 µl by enlarging the bore of the sample channel to 0.0225″. This injection volume ensured a chromatographic peak-width at half-height of about 45 s, adequate for acquiring three spectra under the flow and scanning conditions used. A fused silica capillary (∼3-ft long, 50 µm ID, 400 µm OD, RESTEC) led the CF-FAB supporting fluid (10% glycerol + 10% methanol + 80% dH_2O) from the injector to the probe tip. The outstanding length of the capillary above the stainless steel probe tip surface was adjusted (0.1–0.3 mm) until stable ion peaks were observed on the oscilloscope. A 2.5-cm long, 3-mm wide filter paper strip coiled around the probe tip greatly increased the spectral stability. The supporting fluid to the injector was supplied by a syringe pump (model 100D; Isco Inc., Lincoln, NE), through a PEEK tubing (1/16″ OD, 0.010″ ID) with a rate of 4 µl/min that required a pump pressure of ∼200 psi, and resulted in a source pressure of 3 × 10^{-4} mbar (2.5 × 10^{-1} mbar at the source fore pump).

The MS source temperature was kept at 45°C, and the source potential (the ion accelerating voltage) at 6 kV. Xenon was used for the generation of the fast atom beam of 6 kV energy and 1 mA intensity. Positive ion mass spectra were recorded in the mass range of 240–3,500 D and with a scan rate of 10 s/decade (∼20 s/scan).

Tandem MS/MS Spectrometry. For obtaining MS/MS spectra, the first (sector) MS was focused to transmit the precursor (parent) ion selected from the primary mass spectrum. The ICP (Instrument Control Parameters) program module of the data system was used in this process, and it required one injection of the sample. After focusing the sector MS, the ion signals from the second (dual quadrupole) MS were observed: the transmission of the parent ion and the occurrence of the product ions were checked on the oscilloscope. The resolution, analyzer-energy (pole-bias) and collision-energy dials were slightly adjusted when finer tuning seemed to be necessary; the double quad unit was basically optimized before the continuous flow experiments, under static FAB-MS conditions. Argon was used as a collision gas, and its flow was adjusted to decrease the original intensity of the precursor ion by one half. The pressure reading at the ion gauge of the associated diffusion pump was $1 \cdot \times 10^{-6}$ mbar. The collision energy was between 38 and 48 V. The protonated molecular ion of Leu-Enkephalin (m/z 556) was used for instrument tuning under static FAB-MS conditions, and injections of 100 ng/μl Leu-Enkephalin solution were used to verify the optimal settings for the CF-FAB experiments.

The analyzer quadrupole was scanning with a speed of 5 s/spectrum in the mass range of 100–900 D, and the MS/MS spectra were recorded in MCA (multiple channel analyzer) format: 8–10 continuum spectra at the elution-maximum of the sample were summed, then the resulting spectrum processed (smoothed, peak-detected, and mass converted) in the usual, mass vs. relative abundance, bar diagram format.

MALDI Mass Spectrometry Analysis. Control AA and HDSS β-actin were subjected to mass spectrometric analysis using a matrix-assisted laser desorption time-of-flight mass spectrometer constructed at Rockefeller University (New York, NY) and described elsewhere (Beavis and Chait, 1989, 1990). The mass spectra shown in Fig. 7 were obtained by adding the individual spectra obtained from 200 laser shots. Actin samples were prepared for laser desorption mass analysis as follows. The laser desorption matrix material (4-hydroxy-α-cyano-cinnamic acid) was dissolved in formic acid/water/isopropanol 1:3:2 (vol/vol/vol) to a concentration of 50 mM. A 75 mM ammonium bicarbonate solution (pH 7.8) containing the actin sample was then added to the matrix solution to give a final concentration of the actin of 0.5–1 μM. A small aliquot (0.5 μl) of this mixture was applied to the metal tip of the mass spectrometer sample probe and dried at room temperature. The sample was then inserted into the mass spectrometer and analyzed. Bovine carbonic anhydrase II (29,022 D) was used as an internal calibrant to calibrate the mass spectra.

Synthesis of ^{35}*S-DNPTC.* S-2,4 dinitrophenylthio-[^{35}S]cysteine (^{35}S-DNPTC) was prepared by a modification of previously described protocols (Fontana et al., 1968; Drews and Faulstich, 1990). One mCi (12.5 μmoles) of [^{35}S]cystine (Amersham Corp., Arlington Heights, IL) with a specific activity of 79.1 mCi/mmole and 62.5 μmoles of unlabeled L-cysteine (Aldrich Chemicals) were dissolved in 10 ml of nitrogenated double distilled deionized H$_2$O and the solution adjusted to pH 8.6 with 0.8 M NH$_4$OH. After all crystals had dissolved the solution was stirred under N$_2$ for 2 h at 22°C followed by lyophilization under N$_2$ vapor. Lyophilized crystals were resuspended in 2 ml concentrated formic acid (Sigma Chemicals), mixed with 40.1 mg of 2,4-dinitrobenzenesulfenyl chloride (Aldrich Chem. Co., Milwaukee, WI) freshly dissolved in 2 ml formic acid, and the solution was stirred under N$_2$ for 1.5 h at 22°C. ^{35}S-DNPTC was purified by crystallization from the reaction above by slowly pouring the mixture on 50 ml of dry peroxide free diethyl ether (Aldrich Chem. Co.) with gentle stirring at 22°C for 10 min. Crystals were harvested by centrifugation at 10,300 g for 15 min, washed three times in 50 ml of dry ether, and dried under vacuum. Finally, crystals were resuspended in 20 ml of 10 mM NH$_4$HCO$_3$ and recrystallized overnight at 4°C. Crystals were harvested by centrifugation and dried as described above. The specific activity of the final reagent was ~28 mCi/mmol.

^{35}*S-DNPTC Labeling of* β*-Actin.* β-actin (11.6 μM) was labeled with ^{35}S-DNPTC (140 μM) in 2 mM Tris, 0.2 mM ATP, 0.5 mM NaN$_3$, pH 7.8. After incubation (80 min, 22°C) the absorbance at 408 nm was measured versus a blank containing no actin, and the number of free thiols per mol AA β-actin was ~1.9. In experiments on HDSS β-actin the number of thiols/mole actin was 0. Labeled actin was applied to a Sephadex G-50 column (50 cm × 1.2 cm) and separated from unbound reagent. The column was eluted with 75 mM NH$_4$HCO$_3$, 0.1 mM CaCl$_2$, pH 7.8, 0.5 ml fractions were collected, and OD$_{280}$ measured. The first peak of OD$_{280}$ contained S-([^{35}S]cysteinyl)-β-actin and was concentrated using a centriprep-30 concentrator to 2.3 μM. The S-([^{35}S]cysteinyl)-β-actin was incubated with 700 μM NEM for 30 min at 22°C, digested with 50/1 trypsin, concentrated and dried, and applied to reverse phase HPLC as described above.

Peptide Synthesis and ^{35}*S-DNPTC Labeling.* Peptides representing fragments of actin generated by digestion with trypsin which contain cysteine residues were synthesized on solid phase using FMOC chemistry. Defined sequence of amino acids were assembled on a 431A peptide synthesizer (Applied Biosystems, Foster City, CA). TFA cleavage was used in conjunction with the appropriate chemical scavengers. Following synthesis, 100 μg of each peptide was purified by reverse phase HPLC (System Gold; Beckman Instruments, Palo Alto, CA), using a standard 0.1% TFA and 80% acetonitrile in 0.1% TFA gradient. After purification peptides were labeled with 10-fold excess S-2,4 dinitrophenylthio [^{35}S]cysteine (^{35}S-DNPTC) by a modification of previously described protocols (Fontana et al., 1968; Drewes and Faulstich, 1990). The reaction of ^{35}S-DNPTC with free reactive thiols could be followed spectrophotometrically since equivalent amounts of yellow 2,4-dinitrothiophenolate was released. Labeled peptides were again separated by reverse phase HPLC as above. After separation 50 μl of each fraction was mixed with 5 ml of liquid scintillation fluid and radioactivity measured (LKB Instruments, Bromma, Sweden). Fractions containing the highest counts were dried (Speed-Vac; Savant Instruments, Inc., Farmingdale, NY) and processed for mass spectroscopy.

Molecular Modeling of Cysteine[284]*-Cysteine*[373] *Disulfide Bond Formation in ISC* β *Actin.* To model the disulfide bond formation between residues 373 and 284 of ISC β-actin, the chaperon portion of the crystal structure profillin-β-actin (Schutt et al., 1993) was removed, hydrogen atoms were added to the remaining structure, and bond orders were assigned. This full atom protein model served as the initial structure for constrained molecular dynamics (MD) simulations. Using a physically relevant set of parameters to represent the potential and kinetic energy of the actin protein model (class II force field; CFF91 [Maple et al., 1990]), molecular dynamics affords conformational exploration across many local minima and maxima in an effort to obtain a globally realistic protein conformation as the CYS-373, CYS-284 distance was closed from 21 to 3 Å. The simulated temperature of the MD simulations was 300°K. Further details concerning our MD simulation methods will appear in a complete article on this subject (Gussio, R., N. Pattabiraman, C. A. Monteiro, and S. R. Goodman, manuscript in preparation).

Results

ISC Core Skeletons Retain The Sickled Shape and Dissociate at A Slower Rate at 37°C Than Do RSC or Control Core Skeletons

The purpose of our studies was to determine why the membrane skeleton released from an ISC, by Triton X-100 extraction, appears unable to remodel to a round or biconcave shape. In their classic studies, Lux and colleagues demonstrated that ISCs extracted in 0.5% Triton X-100 in 56 mM Na Borate, pH 8.0 (30 min, 0°C), yielded skeletons that remained sickled. At the ionic strength used by Lux et al. (1976), spectrin, actin, and protein 4.1 accounted for ~85% of the Coomassie blue–stained protein observed in the skeletons; the remaining proteins being ankyrin, band3, band 4.2, and the other accessory proteins discussed in the introduction. By repeating these experiments under the high ionic strength buffer conditions (10 mM NaPO$_4$, 0.6 M KCl, 1 mM ATP, 1 mM DFP, pH 7.6, + 1% Triton X-100) of Sheetz (1979) we could analyze ISC, RSC, and control core skeletons which maintain the physiological skeletal protein contacts with 95% of lipid extracted (Byers and Branton, 1985; Shen et al., 1986; Liu et al., 1987) and contain almost exclusively spectrin, protein 4.1, and actin.

RBCs from control (AA) subjects and homozygous sickle cell subjects (SS) were separated by a percoll density step gradient. AA core skeletons, low density SS (LDSS) core skeletons, and high density SS (HDSS) core skeletons were prepared by extraction of ghosts in the high ionic strength Triton buffer, and their shape analyzed by indirect immunofluorescence with spectrin antibodies (Fig. 1, *A–C*) and
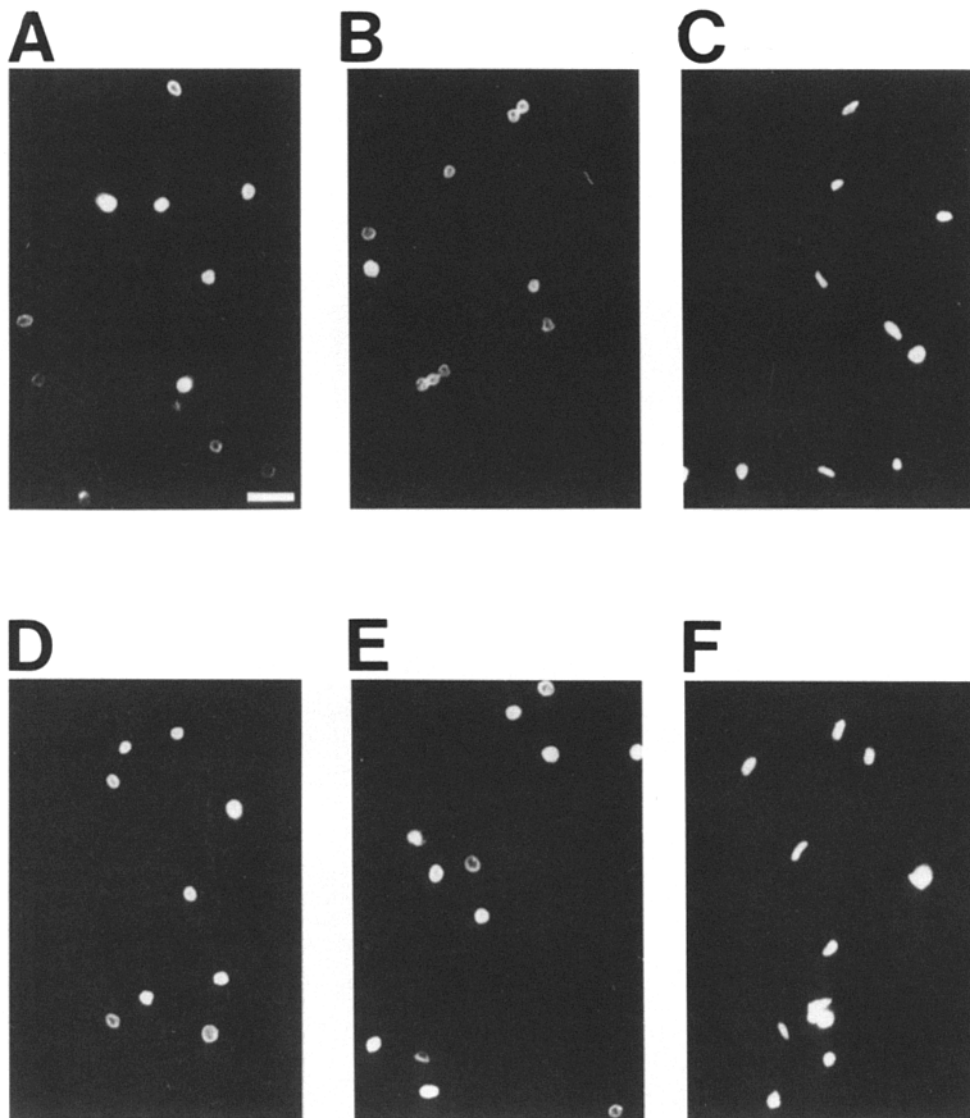
Figure 1. Indirect immunofluorescence of RBC core skeletons. Core skeletons prepared as described in the Materials and Methods section were applied to polylysine-coated glass slides, fixed, and stained with rabbit anti–human rbc spectrin (*A*, *B*, and *C*) and rabbit anti–chicken skeletal muscle actin (*D*, *E*, and *F*) at 1:100 dilution. Fluorescein-conjugated goat anti–rabbit IgG was used in a 1:100 dilution. *A* and *D* are control core skeletons from AA erythrocytes isolated from the 45% Percoll layer. *B* and *E* are core skeletons from the LDSS erythrocytes isolated from the 45% Percoll layer. *C* and *F* are core skeletons from the HDSS erythrocytes isolated from the 65%/70% Percoll layers. Bar, 10 μm.

actin antibodies (Fig. 1, *D–F*). The control AA core skeletons all appeared biconcave or rounded (Fig. 1 *A* and *D*), as did the low density SS core skeletons derived primarily from RSCs (Fig. 1, *B* and *E*). HDSS core skeletons remained almost exclusively sickled in shape because of the high percentage of ISCs in the 65/70% percoll fractions used (Fig. 1, *C* and *F*). The small number of rounded HDSS cores skeletons (15–30%) were probably generated from the USDs (Kaul et al., 1983). We concluded from this study that the defect leading to the persistently sickled ISC membrane skeleton should be found within the core skeleton proteins: spectrin, protein 4.1, or actin, and that RSC core skeletons are capable of remodelling to a biconcave or rounded shape.

SDS-PAGE analysis of ghost protein from AA erythrocytes isolated from 45 and 50% Percoll layers (Fig. 2, *left*, *A*, lanes *a* and *b*) and SS erythrocytes from 45, 50, 55, 60, 65, 70% Percoll layers (Fig. 2, *left*, *A*, lanes *c–h*) indicated no differences in membrane protein composition. Core skeletons prepared by a 15-min extraction at 4°C in high ionic strength Triton buffer demonstrated the presence of

spectrin, protein 4.1 and actin in the control and SS core skeleton samples (Fig. 2, *left*, *B*). All other proteins, including protein 4.9, were present at very low substiochiometric levels. Densitometry of the core skeletons prepared at 4°C indicated that the composition of spectrin, protein 4.1 and actin were nearly identical in AA and SS core skeletons independent of the density of the AA and SS erythrocytes from which they were extracted (Fig. 2, *right*, *top*).

Major differences in the stability of AA and SS core skeletons were observed when the extraction was conducted at 37°C for 15 min in a water jacketed air/CO_2 incubator. As can be clearly seen in Fig. 2 (*left*, *C*, lanes *a* and *b*) and Fig. 2 (*right*, *bottom*) at 37°C (15 min) the control AA core skeletons are greater than 80% dissociated in agreement with the previous results of Yu et al. (1973). Nearly identical results were obtained in separate experiments where the control erythrocytes were obtained from a 35-y-old African American male or a 40-y-old Caucasian male. However the highest density SS cells (65%, 70% Percoll, enriched in ISCs) produced core skeletons where greater than 60% of the spec-
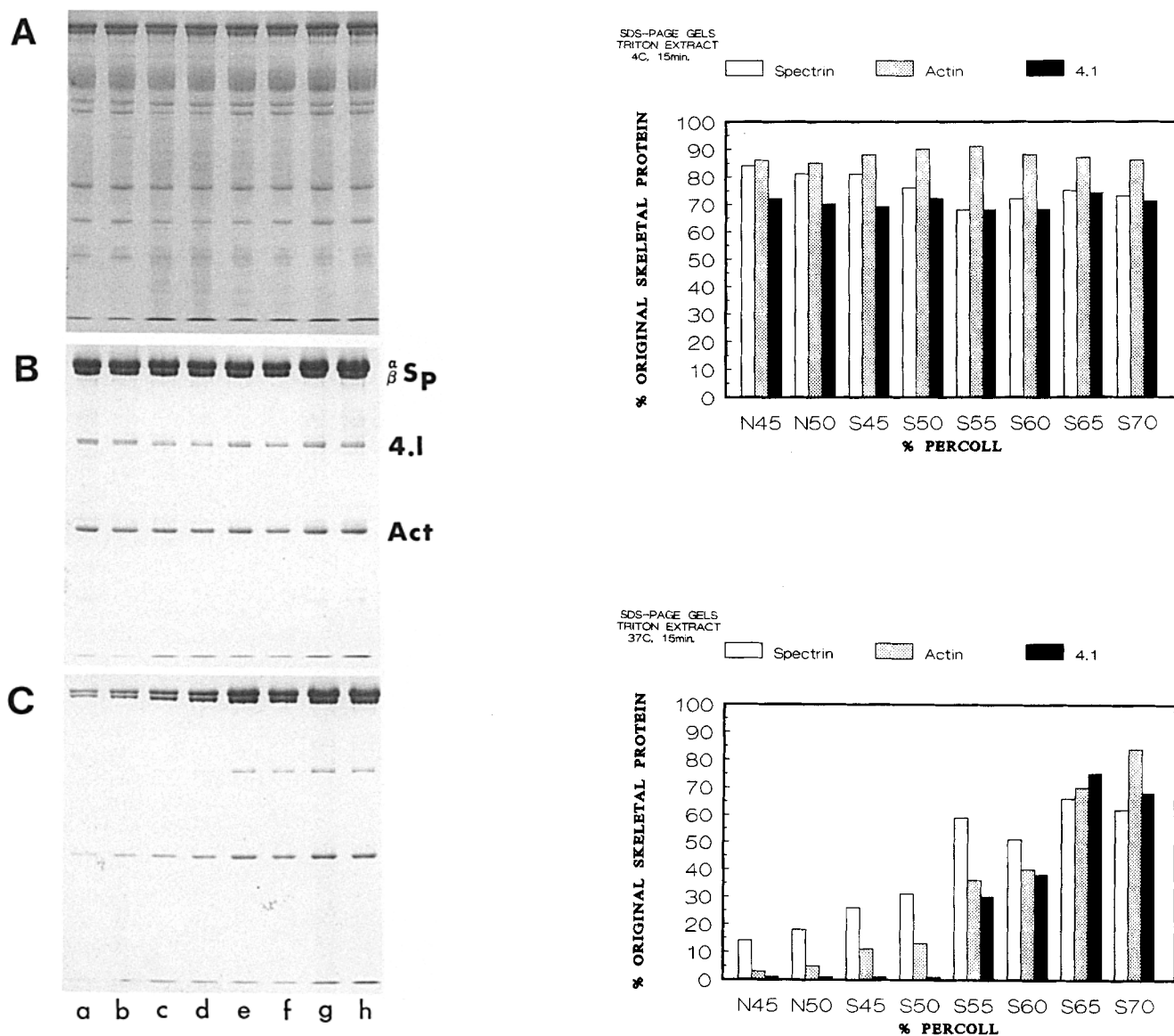
Figure 2. SDS-PAGE of density separated AA and SS erythrocyte ghosts and core skeletons prepared at 4° and 37°C. (*Left*) Coomassie blue stained SDS-PAGE of 20 µl packed rbc ghosts (*A*), core skeletons prepared from 40 µl of packed rbs ghosts by high ionic strength Triton X-100 extraction at 4°C (15 min) (*B*), or 37°C (15 min) (*C*). The source of the material in each lane is AA erythrocytes 45% percoll (lane *a*) and 50% percoll (lane *b*), and SS erythrocytes 45% (lane *c*), 50% (lane *d*), 55% (lane *e*), 60% (lane *f*), 65% (lane *g*), 70% (lane *h*) percoll. (*Right top*) Densitometric analysis of the protein content of core skeletons prepared at 4°C from the SDS-PAGE shown in the left, panel *B.* The content of spectrin, actin, and protein 4.1 is given as % original skeletal protein remaining from the initial ghost protein. *N*, AA normal core skeletons; and *S*, SS core skeletons. x axis is percentage percoll gradient. (*Right, bottom*) Densitometric analysis of the protein content of core skeleton prepared at 37°C from the SDS-PAGE shown in *left,* panel *C.*

trin, protein 4.1, and actin remained associated after 15 min at 37°C (Fig. 2, *left, C,* lanes *g* and *h*). LDSS core skeletons dissociated at a similar rate to AA core skeletons (compare Fig. 2, *left, C,* lanes *c* and *a*). The resistance of SS core skeletons to dissociation at 37°C increased with increasing density of the isolated erythrocytes (Fig. 2, *right, bottom*). Only small density dependent increases in resistance to dissociation were observed for control erythrocytes (Fig. 2, *left, C,* compare lanes *a* and *b*) and sickle cell trait erythrocytes (data not shown).

This slow dissociation of spectrin, protein 4.1, and actin within the ISC core skeleton was not based on a covalent bond because: (*a*) given sufficient time (>30 min) the high

density SS core skeletons will also disassociate at 37°C, and (*b*) the interactions of spectrin, protein 4.1, and actin within the "locked" ISC skeleton are broken by SDS (Fig. 2, *left,* lanes *g* and *h*). We use the term "locked" to imply that the components of the ISC core skeleton disassemble slowly at 37°C (and therefore the skeleton is less capable of remodelling from its persistently sickled shape). We concluded from these studies that a modification in spectrin, protein 4.1, or actin caused the slower dissociation of the ISC core skeleton, based on a noncovalent locking mechanism. Furthermore we concluded that this locking mechanism could be studied in vitro based on the rate of dissociation of ISC versus control core skeletons at 37°C. While the dissociation experiment

810

under the precise conditions described in the Materials and Methods section (37°C, water jacketed air/CO_2 incubator) and presented in Fig. 2 (*left*, *C*) was performed on two independent sickle cell patients, we have performed similar experiments at 24°C up to 37°C (water bath regulated) on 10 additional SS subjects (Shartava et al., manuscript in preparation). We have found on all 12 SS subjects studied, at all temperatures studied (24°–37°C), that HDSS core skeletons (enriched in ISCs) dissociate more slowly than do LDSS core skeleton (enriched in RSCs), and both have a slower rate of dissociation than AA core skeletons (data not shown).

The In Vitro Ternary Complex Dissociation Assay Allows the Identification of β-Actin and Spectrin as the Functionally Altered Proteins Leading to the Slow Dissociating ISC Ternary Complex

Based on our observation that ISC core skeletons are more resistent to dissociation at 37°C, than control AA or RSC skeletons, we created an in vitro assay to determine the protein(s) leading to the slow dissociation of the ISC skeleton. Spectrin, protein 4.1, and actin were isolated by extraction of core skeletons from AA and HDSS RBCs in 2 M Tris, pH 7.2, at 37°C. The extract was then placed on a Sepharose 4B gel filtration column, which led to the isolation of pure spectrin, protein 4.1, and actin as demonstrated on a typical SDS-PAGE shown in Fig. 3 (*left*). To obtain enough spectrin, protein 4.1, and actin from HDSS erythrocytes for the in vitro ternary complex dissociation assay, the ghosts from two SS patients (20 ml blood each) were combined in each experiment.

Spectrin, protein 4.1, and actin isolated from HDSS and control AA core skeletons (prepared at 4°C) were recombined at final concentrations of 400 μg/ml, 80 μg/ml, and 160 μg/ml respectively in polymerizing buffer (4 mM Tris, 0.2 mM ATP, 0.5 mM $NaNa_3$, 2 mM $MgCl_2$, pH 7.4). (We included only spectrin, protein 4.1 and actin in our assay because these were the components of the released core skeletons from ISCs which retained a sickled shape [Fig. 1] and demonstrated resistance to dissociation at 37°C [Fig. 2]. It is possible that other accessory proteins may also play a role in the slow remodelling of the ISC membrane skeleton in vivo). Under these conditions, and ratio of protein components, spectrin, actin, and protein 4.1 are known to form ternary complexes that resemble their physiological molecular contacts (Cohen et al., 1980); although the supramolecular structures formed appear quite different from negatively stained membrane skeletons. We believe the differences in appearance are due to the role the accessory proteins may play in skeleton assembly and the nature of the spectrin-4.1-actin interaction is basically the same as in the intact skeleton. After incubation (22°C, 1 h) the resulting spectrin-4.1-actin complex was sedimented and then shifted to the high ionic strength Triton X-100 buffer and incubated at 37°C for 30 min to allow dissociation to occur. The remaining ternary complex harvested by 100,000 g centrifugation (30 min) was analyzed by SDS PAGE and laser densitometry (Fig. 3, *right*). Although the initial ternary complexes formed by HDSS and AA spectrin, protein 4.1, and actin were identical (because we used a 1-h incubation which is sufficient time for AA and SS spectrin-4.1-actin ternary complex formation to reach steady state; data not shown),

after shifting the ternary complexes to the high ionic strength Triton X-100 buffer at 37°C, we could again see the expected differences in disassociation at 37°C. The data presented in Fig. 3 (*right*) are the mean ± standard error of three independent experiments which all gave very similar results. When the control spectrin-4.1-actin ternary complex was shifted to 37°C only 28.7 ± 6.4% of the spectrin and 35.0 ± 2.5% of the actin resisted dissociation when compared to the HDSS ternary complex (Fig. 3, *right*). This allowed us to perform the critical mixing-matching experiments where the initial ternary complexes were formed from comixtures of HDSS and AA skeletal proteins. Using this technique we demonstrated that a comixture of AA spectrin, AA actin, and HDSS protein 4.1 formed a ternary complex where only 20.0 ± 6.0% of the spectrin and 28.0 ± 4.6% of the actin resisted dissociation at 37°C. These values are not statistically distinct from that obtained with the control ternary complex and therefore protein 4.1 does not play a role in the slow dissociation of the HDSS ternary complex. It is important to note that although HDSS protein 4.1 is known to contain oxidative damage including conversion of cysteines to cysteic acid (Schwartz et al., 1987), these 4.1 modifications do not contribute to the slow dissociation of the HDSS ternary complex. On the other hand, the comixture of AA spectrin, AA protein 4.1, and HDSS actin formed a ternary complex where 78.3 ± 15.7% of the spectrin and 63.3 ± 15.4% of the actin resisted dissociation at 37°C as compared to the HDSS ternary complex (Fig. 3, *right*). Both of these values are statistically distinct ($P < 0.05$) from the control ternary complex values (28.7 ± 6.4% and 35.0 ± 2.5%) and therefore β-actin was the major culprit in the slow dissociation of the HDSS ternary complex. The comixture of HDSS spectrin, AA protein 4.1, and AA actin yielded a ternary complex where 46.7 ± 11.9% of the spectrin and 61.7 ± 4.8% of the actin resisted dissociation at 37°C. For this complex, where only spectrin came from the HDSS erythrocytes, the difference from the control ternary complex was only significantly different for actin dissociation (Fig. 3, *right*).

We concluded from these experiments that a defect in ISC β-actin was the key determinant of the slowly dissociating ISC skeleton, spectrin also appears to play some role, while protein 4.1 is not responsible for the locking mechanism. Since β-actin was the major determinant of the slow dissociation of the ternary complex under the conditions of our assay, and a much smaller protein than spectrin, we decided to determine the ISC β-actin modification first.

Search for the ISC β-Actin Defect Leads to Modified Cysteines

To determine the posttranslational modifications of ISC β-actin, we first isolated β-actin from AA, HDSS (65 and 70% percoll layers, enriched in ISCs), and LDSS (45 and 50% percoll layers, enriched in RSCs) erythrocytes. The isolated β-actin samples were reduced in a buffer containing DTT (0.2 mM), digested with trypsin (50/1, mol/mol) for 20 h at 37°C, and actin peptides were separated by reverse phase HPLC on a C_{18} column. The resulting peptide maps for HDSS β-actin, LDSS β-actin, and AA β-actin were nearly identical (data not shown). Detailed comparisons of the protein containing HPLC fractions (1–50) for HDSS, LDSS, and AA β-actins by FAB-mass spectrometry (FAB-MS) yielded
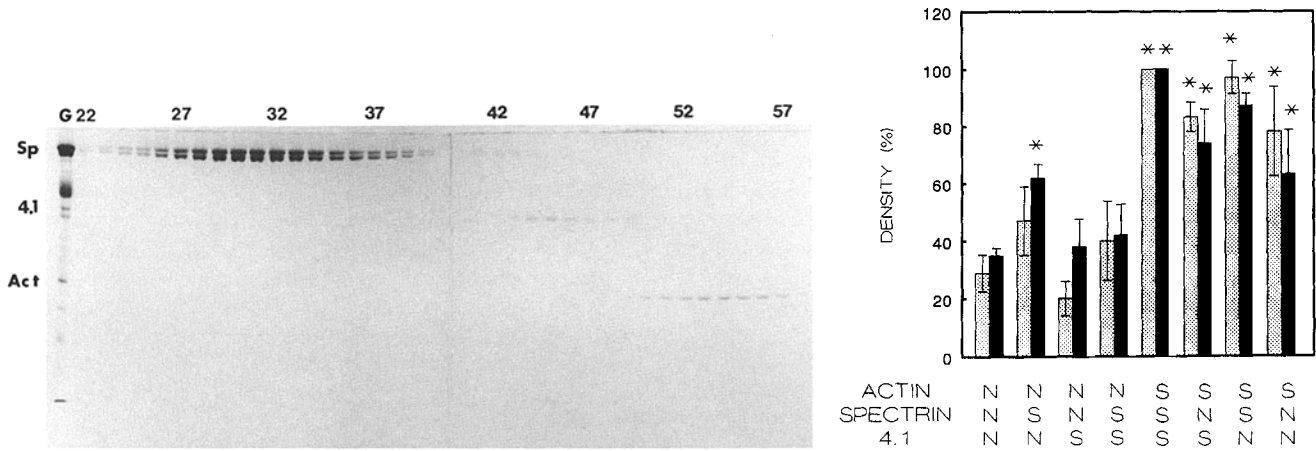
Figure 3. Isolation of core skeleton proteins and in vitro ternary complex dissociation assay. (*Left*) SDS-PAGE of purified spectrin, protein 4.1, and actin isolated by 2 M Tris, pH 7.2, extraction of core skeletons followed by gel filtration on Sepharose 4B. Fraction numbers are given above the gel. (*Right*) Densitometric analysis of the amount of spectrin and actin which resist dissociation at 37°C (30 min) in high ionic strength Triton X-100 buffer, when spectrin-4.1-actin ternary complexes formed in vitro are shifted to these conditions. Details of the protocol are given in the Materials and Methods section. Under each set of bars is given the initial composition of normal AA (*N*) or HDSS (*S*) actin, spectrin, and protein 4.1 in the incubation mixture. The data is expressed as "density %" which indicates the density of spectrin or actin remaining in any complex ÷ density of spectrin or actin remaining in the complex formed by the incubation of HDSS spectrin + HDSS actin + HDSS protein 4.1 × 100%. Data is presented as mean ± standard error, with asterisks indicating a statistically significant difference (*P* <0.05) as compared to the N-Actin/N-Spectrin/N-4.1 sample. Note that HDSS actin forms a ternary complex that is resistant to dissociation even when it has been combined with AA normal spectrin and AA normal protein 4.1. ▨, Spectrin; ■, actin.
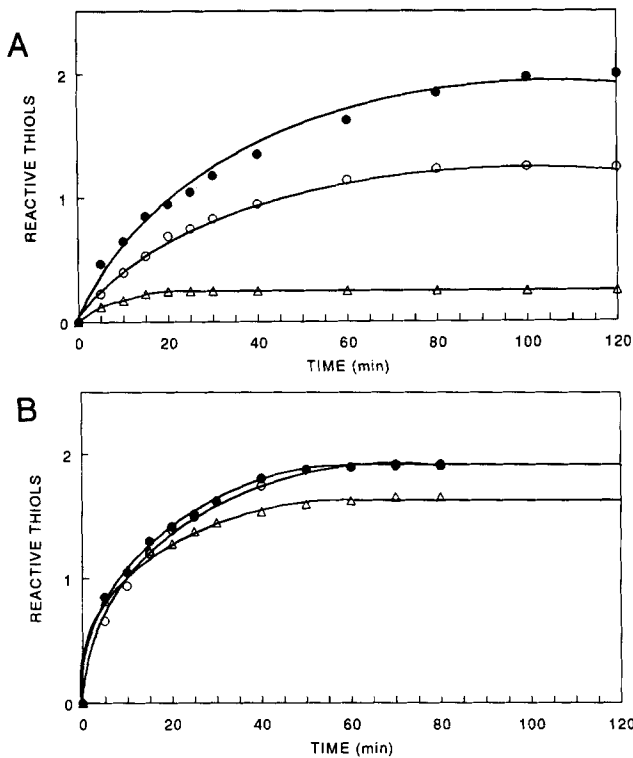

Figure 4. Determination of the number of available thiols in HDSS, LDSS, and AA β-actin. Reduced and nonreduced G-actin (1.5 × 10⁻⁵ M) from control (*AA*), HDSS, and LDSS erythrocytes was incubated with a 10-fold molar excess of DTNB. The reference cuvette contained the actin buffer (2 mM Tris, 0.2 mM ATP, 0.5 mM NaN₃, pH 7.8) plus 1.5 × 10⁻⁴ M DTNB. The color reaction was monitored at 412 nm at 22°C. (*A*) G-actin samples were not reduced. AA actin (●) had 2.0 thiols per mole β actin, LDSS actin (○) had 1.2 thiols per mole β actin, and HDSS actin (△) had 0.2 thiols per mole β actin. (*B*) G-actin samples were reduced with a

virtually identical spectra (data not shown). Of the 38 potential peptides generated by tryptic digestion 20 could be assigned to major ions within our FAB-MS spectra. These 20 tryptic peptide molecular ions were identical in mass when comparing HDSS, LDSS, and control β-actin.

We were now faced with the dilemma of a known functional defect in ISC β-actin with no observable structural change in the tryptic fragments generated from reduced HDSS, LDSS, and AA β-actin. Because of the previous evidence of thiol oxidation in SS membrane skeletal proteins (Rank et al., 1985; Schwartz et al., 1987), we decided to measure the available thiols in nonreduced native β-actin isolated from HDSS, LDSS, and AA erythrocytes (Fig. 4 *A*). Thiol groups available in native β-actin were determined first with 5,5'-dithiobis-(2-nitrobenzoate) (DTNB). As shown in Fig. 4 *A* when the β-actin samples were not incubated with reducing agent, the number of thiols per actin were 2.0 (AA), 1.2 (LDSS), and 0.2 (HDSS) (mol/mol). It now became of substantial interest to determine whether the lack of titratable cysteine residues in HDSS β-actin was reversible upon incubation with reducing agent (DTT). If the β-actin samples were reduced with buffer containing 0.2 mM DTT, and then the DTT removed prior to measurement of thiols with DTNB, then we obtained the results shown in Fig. 4 *B*. With reduced β-actin the number of titratable thiols became 2.0 (AA), 2.0 (LDSS), and 1.6 (HDSS). Therefore the lack of accessible cysteine residues in nonreduced HDSS β-actin was reversible with reducing agent, and therefore could not be explained by oxidation of cysteine to cysteic acid. The

buffer containing 0.2 mM DTT, followed by removal of DTT prior to DTNB measurements of available thiols. Details are given in the Materials and Methods section. Reduced β-actins from AA (●) and LDSS (○) erythrocytes contained 2.0 thiols per mole actin, and β-actin from HDSS (△) erythrocytes had 1.6 thiols per mole actin.
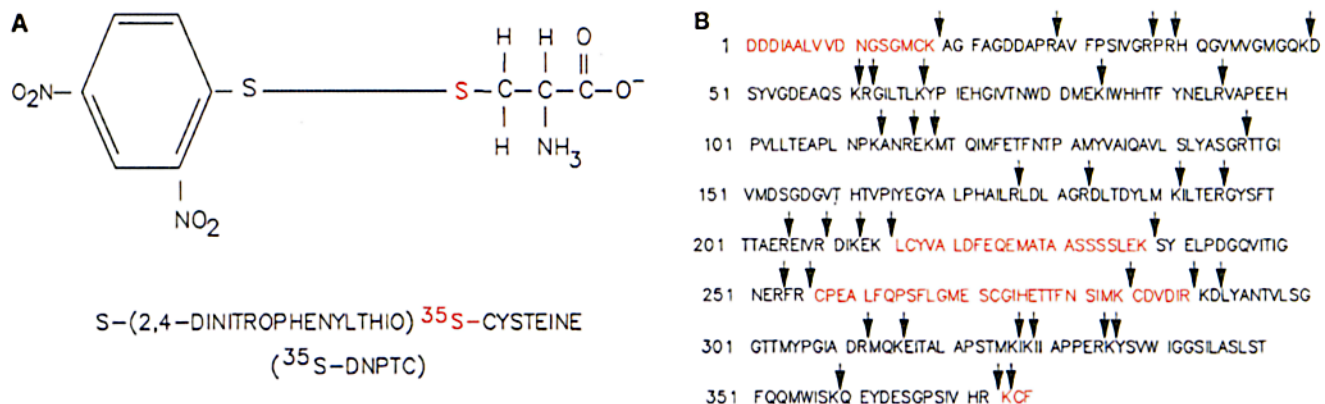
812

A

O$_2$N—(benzene)—S————S—C—C—C—O$^-$

with H H O / H NH$_3$ substituents

S-(2,4-DINITROPHENYLTHIO) ^{35}S—CYSTEINE
(^{35}S-DNPTC)

B

```
  1  DDDIAALVVD NGSGMCK AG FAGDDAPRAV FPSIVGRPRH QGVMVGMGQKD
 51  SYVGDEAQS KRGILTLKYP IEHGIVTNWD DMEKIWHHTF YNELRVAPEEH
101  PVLLTEAPL NPKANREKMT QIMFETFNTP AMYVAIQAVL SLYASGRTTGI
151  VMDSGDGVT HTVPIYEGYA LPHAILRLDL AGRDLTDYLM KILTERGYSFT
201  TTAEREIVR DIKEK LCYVA LDFEQEMATA ASSSSLEK SY ELPDGQVITIG
251  NERFR CPEA LFQPSFLGME SCGIHETTFN SIMK CDVDIR KDLYANTVLSG
301  GTTMYPGIA DRMQKEITAL APSTMKIKII APPERKYSVW IGGSILASLST
351  FQQMWISKQ EYDESGPSIV HR KCF
```

Figure 5. Structure of ^{35}S-DNPTC and β-actin. (*Left*) The structure of S-(2,4-dinitrophenylthio[^{35}S]cysteine) or ^{35}S-DNPTC is presented. The radioactive sulfur is shown in *red*. (*Right*) The primary structure of β-actin is presented using the single letter code for amino acids. The arrows indicate sites of trypsin cleavage. Stretches of amino acids in *red* indicate tryptic peptides which contain cysteine residues. K^{372} is in *red* because under our conditions cleavage after K^{372} occurs less frequently than cleavage after R^{371}, therefore KCF is generated.

most reasonable explanation of these results is that a disulfide bridge is present between two of the six cysteine residues in HDSS (enriched in ISC) β-actin which is not present in control AA β-actin; an alternative explanation being that the two cysteines are blocked by some other mechanism that is reversible with DTT. The determination of exposed thiols with DTNB was performed twice with β-actin samples from four SS subjects with virtually identical results. Furthermore the same results were obtained when S-2,4,dinitrophenylthio[^{35}S]cysteine (^{35}S-DNPTC) (Fig. 5, *left*) was used as the thiol reactive reagent.

Next we wanted to identify the two cysteines which were available to labeling by ^{35}S-DNPTC in AA β-actin but unavailable in nonreduced HDSS β-actin. We began by synthesizing S-(2,4-dinitrophenylthio) [^{35}S]cysteine (^{35}S-DNPTC) which has previously been demonstrated to specifically label exposed thiols utilizing skeletal muscle actin as substrate (Fontana et al., 1968; Drewes and Faulstich, 1990). The advantage of this reagent is that it: (*a*) introduces by disulfide exchange [^{35}S]cysteine as a label to exposed thiols within actin; (*b*) these [^{35}S]cysteinyl-peptide bonds are not broken during trypsin digestion or reverse phase HPLC; (*c*) the addition of the [^{35}S]cysteinyl residue does not change the elution properties of peptides perceivably in reverse phase HPLC, as preliminary experiments with the model peptides demonstrated; and (*d*) the release of 2,3-dinitrothiophenolate allows the efficacy of labeling to be followed by absorbance at 408 nm. The entire sequence of human β-actin is known (Fig. 5, *right*), and it contains six cysteine residues at residues 16, 216, 256, 271, 284, and 373. (In the nomenclature of Vandekerckhove and Weber [1978] these six

β-actin cysteines are numbered 17, 217, 257, 272, 285, and 374 based on alignment with the α-skeletal muscle actin sequence.) Based on the known sequence there should be five tryptic peptides within β-actin which contain cysteine residues (shown in red in Fig. 5, *right*). We synthesized six cysteine containing synthetic peptides shown in Table I. We synthesized both KCF (372–374) and CF (373–374) because it was not clear whether trypsin would cleave at both R^{371} and K^{372} under our digestion conditions. The strategy behind our experiments was that ^{35}S-DNPTC should label two cysteines in AA β-actin and after trypsin digestion and reverse phase HPLC should yield two radiolabeled tryptic peptides which will coelute with two S-([^{35}S]cysteinyl)-synthetic peptides. Furthermore the ^{35}S-cysteinyl-labeled tryptic and synthetic peptides eluted from reverse phase HPLC should contain predicted molecular mass ions (Table I) on FAB-MS.

The results of the experimental approach described above are presented in Figure 6. We labeled AA β-actin with ^{35}S-DNPTC, digested with trypsin, separated the tryptic fragments by reverse phase HPLC, and determined radioactivity in the fractions. Control AA β-actin had two S([^{35}S]cysteinyl)-tryptic peptides, eluting at fractions 17/18 and 21 (Fig. 6, *left*). The broad low peak in fractions 41–56 represents labeling of trypsin because it was observed in control samples which contained trypsin but no β-actin. HDSS actin labeled with ^{35}S-DNPTC, digested with trypsin, and separated on reverse phase HPLC, demonstrated no labeling of tryptic peptides as expected (data not shown). Of the six cysteine containing synthetic peptides, shown in Table I, only residues 1–17, 284–289, 372–374, and 373–374 were soluble in our aqueous buffers. When these soluble syn-

Table I. Cysteine Containing Peptides

Peptide sequence	Residues	[M + H]$^+$	S-([^{35}S]cysteinyl)-[M + H]$^+$
CF	373–374	269	388
KCF	372–374	397	516
CDVDIR	284–289	720	839
DDDIAALVVDNGSGMCK	1–17	1,723	1,842
LCYVALDFEQEMATAASSSSLEK	215–237	2,494	2,613
CPEALFQPSFLGMESCGIHETTFNSIMK	256–283	3,119	3,238

thetic peptides were labelled with ^{35}S-DNPTC and injected into reverse phase HPLC S-([^{35}S]cysteinyl)-^{372}KCF^{374} and S-([^{35}S]-cysteinyl)-^{373}CD^{374} eluted in fractions 17/18 (S-([^{35}S]cysteinyl)-KCF is shown in Fig. 6, left). S-([^{35}S]-cysteinyl)-^{254}CDVDIR^{289} eluted at fraction 21, and S-([^{35}S]-cysteinyl)-^{1}DDDIAALVVDNGSGMCK^{17} eluted at fraction 36. We concluded from the reverse phase HPLC elution, shown in Fig. 6, left, that the two tryptic peptides labeled with ^{35}S-DNPTC in AA β-actin are probably KCF (or CF) and CDVDIR. That this conclusion is correct is demonstrated by the FAB-MS spectra shown in Fig. 6 (right). Fraction 17 from ^{35}S-DNPTC–labeled synthetic KCF (Fig. 6, right, A) and labeled AA β-actin tryptic peptides (Fig. 6, right, B) yielded molecular ions of 397 and 516 on FAB-MS spectrum. The molecular ion of 397 corresponds to [M+H]$^+$ for KCF and 516 represents [M+H]$^+$ for S-([^{35}S]cysteinyl)-KCF. The identification of the molecular ion of 516 as S-([^{35}S]cysteinyl)-KCF was further confirmed by MS/MS tandem spectroscopy (data not shown). Fraction 21 from ^{35}S-DNPTC–labeled synthetic CDVDIR (Fig. 6, right, C) and labeled β-actin tryptic peptides (Fig. 6, right, D) yielded molecular ions at 720 and 839 on FAB-MS spectrum. The molecular ion at 720 corresponds to [M+H]$^+$ for CDVDIR and 839 represents [M+H]$^+$ for S-([^{35}S]cysteinyl)-CDVDIR. We concluded from these studies that the two cysteines which are labeled with thiol reactive reagents are

C^{284} and C^{373} of control AA β-actin. These cysteines are not available in HDSS β-actin, unless this actin is pretreated with reducing agent.

The most reasonable conclusion from our studies was that in HDSS β-actin (highly enriched in ISC β-actin) a disulfide bridge exists between cysteine^{284} and cysteine^{373} making these cysteines unavailable for reaction with DTNB or ^{35}S-DNPTC. Upon reduction with DTT the disulfide bridge is broken, making HDSS β-actin like AA β-actin in having approximately two accessible thiols per actin molecule. While this is the most plausible explanation for our data, it was possible that some other posttranslational modification of ISC β-actin could cause a burying of cysteine^{284} and cysteine^{373}. This modification would have to be reversible with reducing agent, and evaded detection in our previous FAB-MS analysis of tryptic fragments of HDSS versus AA β-actin. While this was a less likely scenario, it could be tested by matrix-assisted laser desorption ionization (MALDI) with a time of flight (TOF) instrument. We measured the molecular weight of nonreduced AA β-actin and HDSS β-actin (Fig. 7, A and B, respectively) by MALDI-TOF mass spectroscopy. The molecular weights were identical within the accuracy of the measurement: 41,760 $\pm$ 100 daltons (HDSS β-actin) and 41,690, $\pm$ 100 D (AA β-actin). These results are consistent with a modification that altered the molecular weight by less than 100 D. Formation of a disulfide bridge, which would
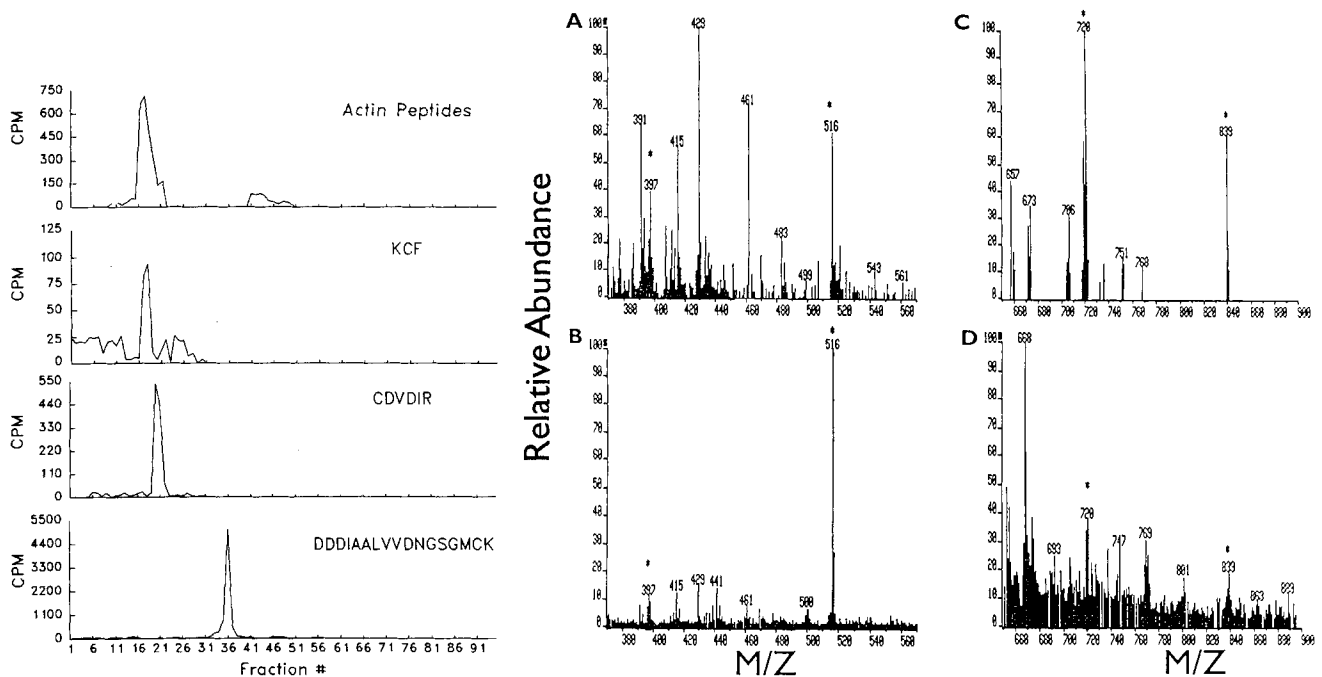
Figure 6. Demonstration that cysteine^{284} within CDVDIR and cysteine^{373} within KCF are the reactive thiols in intact AA β-actin. (Left) Intact AA β-actin and synthetic peptides KCF, CDVDIR, and -DDDIAALVVDNGSGMCK were labeled with ^{35}S-DNPTC as described in Materials and Methods. S-([^{35}S]cysteinyl)-β-actin was cleaved with trypsin and the resulting S-([^{35}S]cysteinyl)-actin peptides were separated by reverse phase HPLC and 50 μl of each fraction was measured for radioactivity. S-([^{35}S]cysteinyl)-KCF, -CDVDIR, and -DDDIAALVVDNGSGMCK were injected into the identical C$_{18}$ column and separated by reverse phase HPLC. Again 50 μl of each fraction was counted for radioactivity. The S-([^{35}S]cysteinyl)-actin peptide peaks in fraction 17/18 and fraction 21, elute in the same position as the synthetic S-([^{35}S]cysteinyl)-KCF and synthetic S-([^{35}S]cysteinyl)-CDVDIR. (Right) FAB-MS was conducted on fraction 17 from the reverse phase HPLC separation of synthetic S-([^{35}S]cysteinyl)-KCF (A) and fraction 17 from S-([^{35}S]cysteinyl)-actin peptides (B). The molecular ions with asterisks are KCF (397) and S-([^{35}S]cysteinyl)-KCF (516). FAB-MS was also conducted on fraction 21 from the reverse phase HPLC separation of synthetic S-([^{35}S]cysteinyl)-CDVDIR (C) and fraction 21 from S-([^{35}S]cysteinyl)-actin peptides (D). The molecular ions with asterisks are CDVDIR (720) and S-([^{35}S]cysteinyl)-CDVDIR (839).
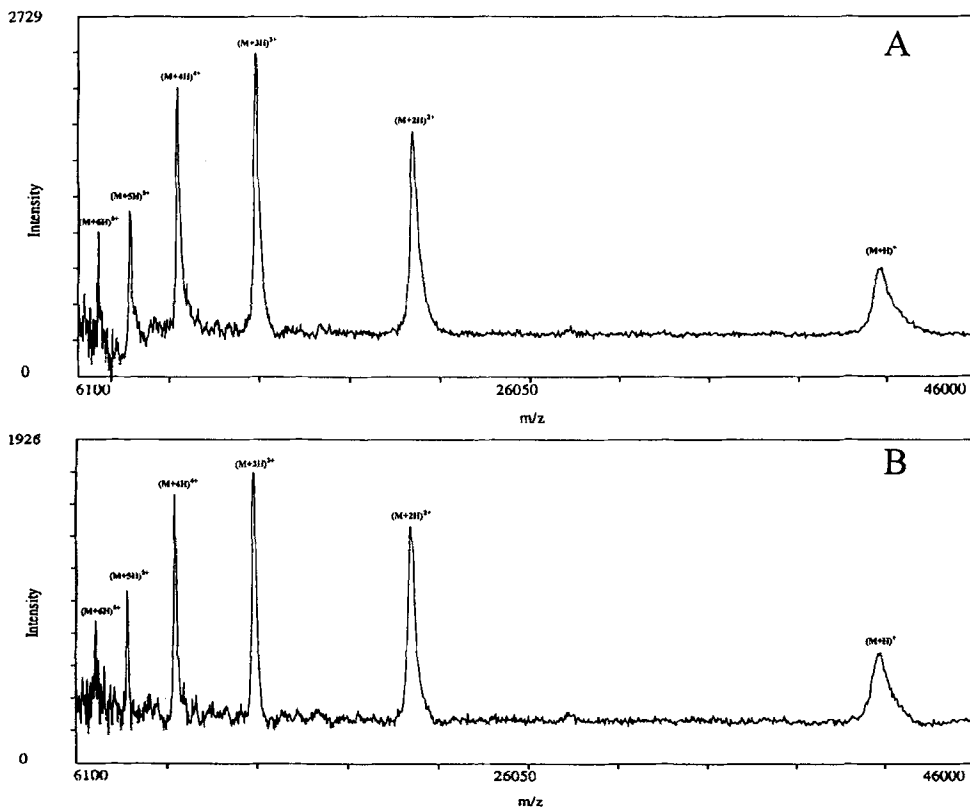
2729

1926

Figure 7. Molecular weight determination of β-actin from MALDI-TOF spectra. MALDI-TOF mass spectra of β-actin isolated from control AA erythrocytes (*A*) and HDSS erythrocytes (*B*). The molecular weights were 41,690 ± 100 and 41,760 ± 100, respectively.

cause a change of only 2 mass units, certainly falls within this range. If any other modification exists it would have to change the molecular weight of the protein by less than 100 mass units. The experimentally determined molecular weights of HDSS and AA β-actin are consistent within the error of measurement with the molecular weight calculated from the known amino acid sequence (41,605.6 D) plus D[1] acetylation (42 D) and H[72] methylation (14 D) (Nakajima-Iijima et al., 1985).

Discussion

Based on our functional assays, we have demonstrated that a modification of β-actin is the major determinant of the slow dissociation of the ISC membrane skeleton. It is logical extension of our work that slower dissociation of the ISC core skeleton is probably responsible for the slow remodelling of the ISC skeleton and hence its persistently sickled shape upon release from the lipid bilayer. Other accessory membrane skeletal proteins, as well as cytoplasmic factors, may also contribute to the inability of the ISC to change shape in vivo.

Furthermore we demonstrate that a posttranslational modification differentiates ISC (or HDSS) β-actin from control β-actin; which is probably a disulfide bridge between cysteine[284] and cysteine[373]. This latter conclusion is supported by the following observations: (*a*) The amount of available thiols is ~2 mol/mol (AA β-actin) and 0 mol/mol (HDSS β-actin) for nonreduced samples, but becomes 2 mol/mol (AA) and close to 2 mol/mol (HDSS) when β-actin is reduced with DTT. (*b*) No difference between reduced HDSS and AA β-actin tryptic peptides could be detected by

HPLC-FAB-MS. (*c*) The molecular weights of nonreduced HDSS and AA β-actin are identical (41,760 ± 100 D versus 41,690 ± 100 D) or within 100 mass units of each other. (*d*) Cysteine[284] and cysteine[373] can be labeled by [32]S-DNPTC in the intact AA β-actin molecule but not in the HDSS (or ISC) β-actin molecule. (*e*) MALDI mass spectrometric peptide mapping experiments using V8-protease, endoproteinase Lys-C and endoproteinase Asp-N did not show any unknown modification in HDSS actin compared to AA actin within the observed part of the sequence (~90%) (Schneider and Chait, unpublished results).

Although β-actin is a major determinant of the ISC skeleton locking mechanism, as determined by our in vitro ternary complex dissociation assay, spectrin also may play a role. Liu et al. (1993) have recently suggested that the spectrin dimer–tetramer equilibrium may play a role in the permanent deformation of irreversibly sickled cells. They base their conclusion on the fact that RSCs could be converted to ISCs in vitro at 37°C, a temperature at which spectrin tetramer–dimer interconversion occurs in solution, but RSCs were not converted to ISCs at 13°C, a temperature at which tetramer–dimer interconversion does not occur. The possibility that spectrin reorganization may be involved in the permanent deformation of the ISC membrane skeleton is intriguing, and not in conflict with our current experiments. The current data showing that a modification of β-actin contributes to slower dissociation of ISC versus AA core skeletons at 37°C, suggests that the temperature dependence of actin polymerization and depolymerization at 37 and 13°C must also be considered to interpret the findings of Liu et al. (1993). It is also important to point out that our data deals with the question of why the ISC skeleton remains sickled

upon release from the membrane, and does not address the question of whether the persistently sickled skeleton was imprinted by an abnormal membrane or vice versa.

It will be of great interest to determine the effect of the predicted cysteine[284]-cysteine[373] intramolecular disulfide bond (or alternative block of these cysteines) upon ISC β-actin structure and its interactions with spectrin and other actin monomers. Our data suggests that the structural modification of ISC β actin would lead to a higher affinity noncovalent interaction with spectrin, other actin monomers, or both. Consistent with this concept, Lux and John (1978) have demonstrated that ISC ghosts could be converted to a round echinocytic shape, after a lag period, by a 20-min incubation in 600 mM NaCl at 37°C. We have recently found that when ISC core skeletons are incubated in the high ionic strength Triton X-100 buffer in a 37°C water bath (instead of the 37°C water jacked air/CO$_2$ incubator used in the current study) that 20 min is sufficient time to obtain extensive dissociation (Shartava, A., P. Miranda, A. Shah, C. A. Montiero, and S. R. Goodman, manuscript in preparation). (This is due to the fact that the samples reach the designated temperature [37°C] more rapidly in the water bath than in an air/CO$_2$ incubator.) Therefore the lag period observed in the conversion of ISC ghosts to rounded echinocyte ghosts at 37°C (Lux and John, 1978) was undoubtedly due to the time required to dissociate the locked ISC skeletons. In the 37°C water bath one still sees the slower rate of ISC versus control core skeleton dissociation (Shartava et al., manuscript in preparation), but both have faster kinetics than observed in the 37°C air/CO$_2$ incubator (presented in Fig. 2). The results of Lux and John (1978), and our current observations, point to the need of a careful evaluation of the ISC versus control actin–actin and actin–spectrin interactions. Comparisons of ISC versus control actin polymerization rates and

the ability of f-actin to bind spectrin $\pm$ protein 4.1, currently underway, will allow us to determine whether the modification of cysteines effects actin/actin or actin/spectrin interactions.

Atomic structural models of g-actin from x-ray crystallography of the α-skeletal muscle actin/DNAse I complex (Kabsch et al., 1990) and bovine β-actin/profilin complex (Schutt et al., 1993) are now available. From these models cysteine[373] in β-actin resides within subdomain I, a region of actin involved in the binding of various actin binding proteins. The β-actin model (Schutt et al., 1993) would place cysteine[284] in subdomain III, with a separation of 21.63 Å between the two sulfur atoms. This indicates that a substantial conformational change in ISC β-actin would be required to allow disulfide bridge formation to occur between cysteine[284] and cysteine[373] (or alternatively that these cysteines are blocked by some other DTT-dependent mechanism which has gone undetected by our mass spectroscopy analysis). The inherent assumption in the existing x-ray crystallography analysis of g-actin (Kabsch et al., 1990; Schutt et al., 1993) is that binding of DNAse or profillin does not alter the structure of actin. But differences in actin structure determined for the actin/DNAse and actin/profillin crystalline structure may indicate that this assumption is not valid. Furthermore, we need to remember that protein structure in solution is dynamic. We have performed extensive computer modeling of the β-actin structure which indicates that the C[284]-C[373] disulfide bond can be formed in solution. Fig. 8 is a stereo view of the backbone of the actin crystal structure and the protein model of the formed C[284]-C[373] disulfide bond. From viewing the figure, one can observe only minor shifts in the tertiary structural domain, which for the most part, occur in the proximity of the ATP binding region (RMS deviation of all backbone atoms = 2.6 Å). It is reasonable
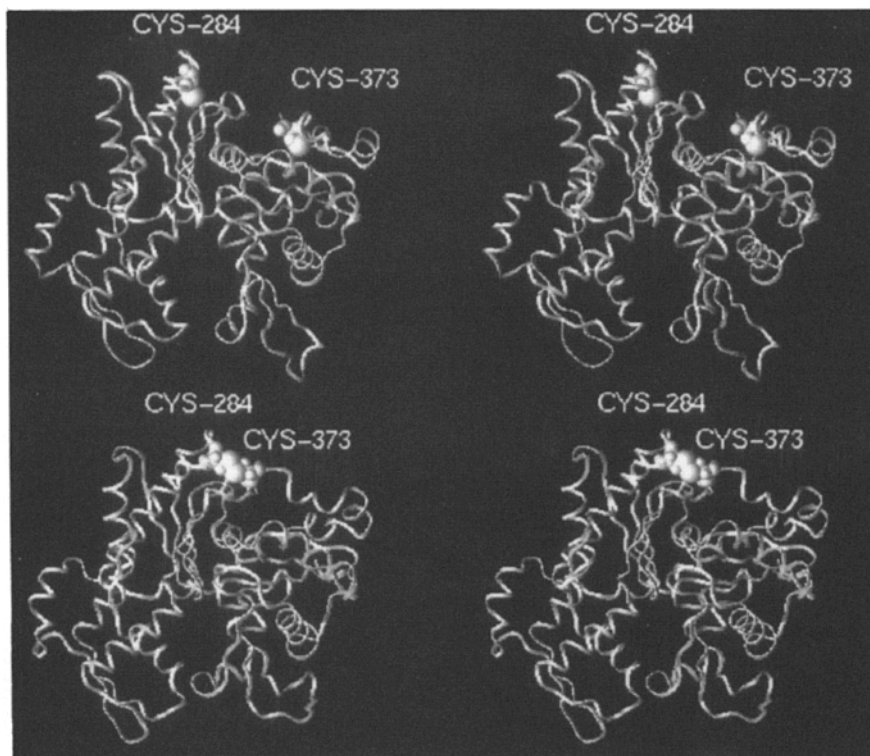
Figure 8. Computer modeling of ISC β-actin. Stereo view of the beta actin crystal structure backbone (*top*) with the profilin chaperon portion removed. In the crystal structure, the CYS 373 and 284 side chain sulfur atoms are 21.63 Å apart. The second model (*bottom*) represents β-actin with the disulfide bridge formed between residues CYS 373 and CYS 284.

that these minor structural changes may not have occurred if an ATP–actin complex structure was used for the molecular modeling simulations. Our model suggests that the carboxy terminal portion of actin (residues 372–374) undergoes a conformational change when its chaperon protein dissociates which orients the C^{373} side chain toward the solvent and predisposes both C^{373} and C^{284} residues to disulfide bond formation. A complete report of our computer modeling of β-actin is currently being prepared (Gussio, R., N. Pattabiraman, C. A. Montiero, and S. R. Goodman, manuscript in preparation). X-ray analysis of β-actin from ISCs and control AA erythrocytes will be required before we can confirm the distances between cysteine^{284} and cysteine^{373} in control rbc β-actin, determine whether the conformational change required for disulfide bridge formation occurs in ISC β-actin, and understand the relationship between the structural changes in β-actin and the functional changes leading towards the "locked" ISC skeleton.

Finally, reduced glutathione levels are diminished about 20% in SS RBCs as compared to high reticulocyte controls, and is lower in ISCs than in RSCs (Lachant et al., 1983; Wetterstroem et al., 1984). The diminished levels of reduced glutathione are related to decreased glutathione reductase activity, increased glutathione peroxidase activity, and inhibition of the pentose phosphate shunt in SS erythrocytes (Lachant et al., 1983). Therefore ISCs have increased activated oxygen species, but decreased levels of reduced glutathione to protect the cell from oxidant damage. The diminished levels of this intracellular reducing agent, probably led to the cysteine oxidation in ISC β-actin. In recent studies we have demonstrated that the membrane permeable reducing agent dithiothreitol blocks the formation of ISCs by in vitro deoxygenation–reoxygenation cycling and converts ISCs isolated from the blood of sickel cell patients to RSCs (Campbell, N. F., Y. Zhang, W. Korn, A. Shartava, and S. R. Goodman, manuscript in preparation). If safe membrane permeable reducing agents can block ISC formation in vivo, then this will suggest future therapeutic interventions to diminish the number of sickle cell crisis episodes and organ damage related to sickle cell anemia.

References

Ballas, S. K., and E. D. Smith. 1992. Red blood cell changes during the evolution of the sickle cell painful crisis. *Blood.* 79:2154–2163.

Ballas, S. K., J. Larner, E. D. Smith, S. Surrey, E. Schwartz, and E. F. Rappaport. 1988. Rheologic predictors of the severity of the painful sickle cell crisis. *Blood.* 72:1216–1223.

Beavis, R. C., and B. T. Chait. 1989. Factors affecting the ultraviolet laser desorption of proteins. *Rapid Commun. Mass Spectrom.* 3:233–237.

Beavis, R. C., and B. T. Chait. 1990. High-accuracy molecular mass determination of proteins using matrix-assisted laser desorption mass spectrometry. *Anal. Chem.* 62:1836–1840.

Bennett, V., and P. J. Stenbuck. 1979. Identification and partial purification of ankryin, the high affinity membrane attachment site for human erythrocyte spectrin. *J. Biol. Chem.* 254:2533–2541.

Bennett, V., and P. J. Stenbuck. 1980. Association between ankyrin and the cytoplasmic domain of band 3 isolated from erythrocyte membrane. *J. Biol. Chem.* 255:6424–6432.

Brenner, S. L., and E. Korn. 1979. Spectrin-actin interaction. Phosphorylated and dephosphorylated spectrin tetramer cross-link f-actin. *J. Biol. Chem.* 254:8620–8627.

Byers, T. J., and D. Branton. 1985. Visualization of the protein associations in the erythrocyte membrane skeleton. *Proc. Natl. Acad. Sci. USA.* 82:6151–6157.

Cohen, C. M., J. M. Tyler, and D. Branton. 1980. Spectrin-actin association studied by electron microscopy of shadowed preparations. *Cell.* 21:875–883.

Drewes, G., and H. Faulstich. 1990. 2, 4-Dinitrophenyl [^{14}C] cysteinyl disulfide allows selective radioactive labelling of protein thiols under spectrophotometric control. *Anal. Biochem.* 188:109–113.

Ellman, G. L. 1958. A colorimetric method for determining low concentrations of mercaptans. *Arch. Biochem. Biophys.* 74:443–450.

Fabry, M. E., L. Benjamin, C. Lawrence, and R. L. Nagel. 1984. An objective sign in painful crisis in sickle cell anemia: the concomitant reduction in high density red cells. *Blood.* 64:559–565.

Fabry, M. E., E. Fine, V. Rajanayagam, S. M. Factor, J. Gore, M. Sylla, and R. L. Nagel. 1992. Demonstration of endothelial adhesion of sickle cells in vivo: a distinct role for deformable sickle cell discocytes. *Blood.* 79:1602–1611.

Fontana, A., E. Scoffone, and C. A. Benassi. 1968. Sulfenyl halides as modifying reagents for polypeptides and proteins. II. Modification of cysteinyl residues. *Biochemistry.* 7:980–986.

Fowler, V., and D. L. Taylor. 1980. Spectrin plus band 4.1 crosslink actin. Regulation by micromolar calcium. *J. Cell Biol.* 85:361–376.

Fowler, V. M., and V. Bennett. 1984. Erythrocyte membrane tropomyosin. *J. Biol. Chem.* 259:5978–5989.

Francis, R. B. Jr., and C. S. Johnson. 1991. Vascular occlusion in sickle cell disease: current concepts and unanswered questions. *Blood.* 77:1405–1414.

Gardner, K., and V. Bennett. 1987. Modulation of spectrin-actin assembly by erythrocyte adducin. *Nature (Lond.).* 328:359–362.

Goodman, S. R., I. S. Zagon, and R. R. Kulikowski. 1981. Identification of a spectrin-like protein in nonerythroid cells. *Proc. Natl. Acad. Sci. USA.* 78:7570–7574.

Goodman, S. R., K. E. Krebs, C. F. Whitfield, B. M. Riederer, and I. S. Zagon. 1988. Spectrin and related molecules. *CRC Crit. Rev. Biochem.* 23:171–234.

Hargreaves, W. R., K. N. Giedd, A. Verkleij, and D. Branton. 1980. Reassociation of ankyrin with band 3 in erythrocyte membranes and in lipid vesicles. *J. Biol. Chem.* 255:11965–11972.

Hebbel, R. P. 1990. The sickle erythrocyte in double jeopardy: autoxidation and iron decompartmentalization. *Semin. Hematol.* 27:51–69.

Hebbel, R. P. 1991. Beyond hemoglobin polymerization: the red blood cell membrane and sickle disease pathophysiology. *Blood.* 77:214–237.

Hebbel, R. P., J. W. Eaton, M. Balasingam, and M. H. Steinberg. 1982. Spontaneous oxygen radical generation by sickle erythrocytes. *J. Clin. Invest.* 70:1253–1259.

Hebbel, R. P., W. T. Morgan, J. W. Eaton, and B. E. Hedlund. 1988. Accelerated autoxidation and heme loss due to instability of sickle hemoglobin. *Proc. Natl. Acad. Sci. USA.* 85:237–242.

Joiner, C. H. 1993. Cation transport and volume regulation in sickle red blood cells. *Am. J. Physiol.* 264:C251–C270.

Kabsch, W., H. G. Mannherz, D. Suck, E. F. Pai, and K. C. Holmes. 1990. Atomic structure of the actin-DNase I complex. *Nature (Lond.).* 347:37–44.

Karinch, A. M., W. E. Zimmer, and S. R. Goodman. 1990. The identification and sequence of the actin-binding domain of human red blood cell β-spectrin. *J. Biol. Chem.* 265:11833–11840.

Kaul, D. K., M. E. Fabry, P. Windisch, S. Baez, and R. L. Nagel. 1983. Erythrocytes in sickle cell anemia are heterogeneous in their rheological and hemodynamic characteristics. *J. Clin. Invest.* 72:22–31.

Kaul, D. K., M. E. Fabry, and R. L. Nagel. 1986. Vaso-occlusion by sickle cells: evidence for selective trapping of dense red cells. *Blood.* 68:1162–1169.

Kaul, D. K., M. E. Fabry, and R. L. Nagel. 1989. Microvascular sites and characteristics of sickle cell adhesion to vascular endothelium in shear flow conditions: pathophysiological implications. *Proc. Natl. Acad. Sci. USA.* 86:3356–3362.

Kuross, S. A., B. H. Rank, and R. P. Hebbel. 1988. Excess heme in sickle erythrocyte inside-out membranes: possible role in thiol oxidation. *Blood.* 71:876–882.

Lachant, N. A., W. D. Davidson, and K. R. Tanaka. 1983. Impaired pentose phosphate shunt function in sickle cell disease: a potential mechanism for increased Heinz body formation and membrane lipid peroxidation. *Am. J. Hematol.* 15:1–13.

Laemmli, U. K. 1970. Cleavage of structural proteins during the assembly of the head of bacteriophage T4. *Nature (Lond.).* 227:680–685.

Lande, W. M., D. L. Andrews, M. R. Clark, N. V. Braham, D. M. Black, S. H. Embury, and W. C. Mentzer. 1988. The incidence of painful crisis in homozygous sickle cell disease: correlation with red cell deformability. *Blood.* 72:2056–2059.

Liu, S. C., L. H. Derick, and J. Palek. 1987. Visualization of the hexagonal lattice in the erythrocyte membrane skeleton. *J. Cell Biol.* 104:527–536.

Liu, S. C., L. H. Derick, and J. Palek. 1993. Dependence of the permanent deformation of red blood cell membranes on spectrin dimer-tetramer equilibrium: implication for permanent membrane deformation of irreversibly sickled cells. *Blood.* 81:522–528.

Lux, S. E., and K. M. John. 1978. The role of spectrin and actin in irreversibly sickled cells: unsickling of "irreversibly" sickled ghosts by conditions which interfere with spectrin-actin polymerization. *In* Biochemical and Clinical Aspects of Hemoglobin Abnormalities. W. S. Caughey, editor. Academic Press, New York, NY. 335–352.

Lux, S. E., K. M. John, and M. J. Karnovsky. 1976. Irreversible deformation of the spectrin-actin lattice in irreversibly sickled cells. *J. Clin. Invest.* 58:955–963.

Maple, J. R., T. S. Thacher, U. Dinur, and A. T. Hagler. 1990. Biosym force field research results in new techniques for the extraction of inter- and intramolecular forces. *Chem. Design Automat. News.* 5(9):5–10.

Mische, S. M., M. S. Mooseker, and J. S. Morrow. 1987. Erythrocyte adducin: a calmodulin-regulated actin-bundling protein that stimulates spectrin-actin binding. *J. Cell Biol.* 105:2837–2845.

Montgomery, D. C. 1991. Design and analysis of experiments. John Wiley & Sons, New York, NY.

Mueller, T. J., and M. Morrison. 1981. Glycoconnectin (PAS 2) a membrane attachment site for the human erythrocyte cytoskeleton. *In* Erythrocyte Membranes 2: Recent Clinical and Experimental Advances. W. C. Kruckeberg, J. W. Eaton, and G. J. Brewer, editors. Alan R. Liss Inc., New York, NY. 95–112.

Nakajima-Iijima, S., H. Hamada, P. Reddy, and T. Kakunaga. 1985. Molecular structure of the human cytoplasmic β-actin gene: interspecies homology of sequences in the introns. *Proc. Natl. Acad. Sci. USA.* 82:6133–6137.

Platt, O. S., J. F. Falcone, and S. E. Lux. 1985. Molecular defect in the sickle erythrocyte skeleton. Abnormal spectrin binding to sickle inside-out vesicles. *J. Clin. Invest.* 75:266–271.

Powers, D. R. 1990. Sickle cell anemia and major organ failure. *Hemoglobin.* 14:573–598.

Rank, B. H., J. Carlsson, and R. P. Hebbel. 1985. Abnormal redox status of membrane-protein thiols in sickle erythrocytes. *J. Clin. Invest.* 75:1531–1537.

Sahr, K. E., P. Laurila, L. Kotula, A. L. Scarpa, E. T. L. Coupal, A. J. Linnenbach, J. C. Winkelmann, D. W. Speicher, V. T. Marchesi, P. J. Curtis, and B. G. Forget. 1990. The complete cDNA and polypeptide sequences of human erythroid α-spectrin. *J. Biol. Chem.* 265:4434–4443.

Schutt, C. E., J. C. Myslik, M. D. Rozycki, N. C. W. Goonesekere, and U. Lindberg. 1993. The structure of crystalline proflin-β-actin. *Nature (Lond.).* 365:810–816.

Schwartz, R. S., A. C. Rybicki, R. H. Heath, and B. H. Lubin. 1987. Protein 4.1 in sickle erythrocytes. Evidence for oxidative damage. *J. Biol. Chem.* 262:15666–15672.

Sheetz, M. P. 1979. Integral membrane protein interactions with triton cytoskeletons of erythrocytes. *Biochim. Biophys. Acta.* 551:122–134.

Shen, B. W., R. Josephs, and T. L. Steck. 1986. Ultrastructure of the intact skeleton of the human erythrocyte membrane. *J. Cell Biol.* 102:997–1006.

Shiffer, K. A., and S. R. Goodman. 1984. Protein 4.1: its association with the human erythrocyte membrane. *Proc. Natl. Acad. Sci. USA.* 81:4404–4408.

Shotton, D., B. E. Burke, and D. Branton. 1979. The molecular structure of human erythrocyte spectrin. Biophysical and electronmicroscopic studies. *J. Mol. Biol.* 131:303–329.

Siegel, D. L., and D. Branton. 1985. Partial purification and characterization of an actin-bundling protein, band 4.9, from human erythrocytes. *J. Cell Biol.* 100:775–785.

Tyler, J. M., W. R. Hargreaves, and D. Branton. 1979. Purification of two spectrin-binding proteins: biochemical and electron microscopic evidence for site specific reassociation between spectrin and bands 2.1 and 4.1. *Proc. Natl. Acad. Sci. USA.* 76:5192–5196.

Ungewickell, E., P. M. Bennett, R. Calvert, V. Ohanian, and W. B. Gratzer. 1979. In vitro formation of a complex between cytoskeletal proteins of the human erythrocyte. *Nature (Lond.).* 280:811–814.

Vandekerckhove, J., and K. Weber. 1978. At least six different actins are expressed in a higher mammal: an analysis based on the amino acid sequence of the amino-terminal tryptic peptide. *J. Mol. Biol.* 126:783–802.

Wallin, R., E. N. Culp, D. B. Coleman, and S. R. Goodman. 1984. A structural model of human erythrocyte band 2.1: alignment of chemical and functional domains. *Proc. Natl. Acad. Sci. USA.* 81:4095–4099.

Wetterstroem, N., G. J. Brewer, J. A. Warth, A. Mitchinson, and K. Near. 1984. Relationship of glutathione levels and Heinz body formation to irreversibly sickled cells in sickle cell anemia. *J. Lab Clin. Med.* 103:589–596.

Winkelmann, J. C., J. G. Chang, W. T. Tse, A. L. Scarpa, V. T. Marchesi, and B. G. Forget. 1990. Full-length sequence of the cDNA for human erythroid β-spectrin. *J. Biol. Chem.* 265:11827–11832.

Yu, J., D. A. Fischman, and T. L. Steck. 1973. Selective solubilization of proteins and phospholipids of red blood cell membranes by nonionic detergents. *J. Supramol. Struct.* 1:233–248.

Yu, J., and S. R. Goodman. 1979. Syndeins: the spectrin-binding protein(s) of the human erythrocyte membrane. *Proc. Natl. Acad. Sci. USA.* 76:2340–2344.